The derivation and application of convective pattern equations

Yiping Ma

Advised by Edward A Spiegel

Abstract

In this report, we review an elegant technique, known as the Bogoliubov method, for deriving amplitude equations in pattern forming systems, through detailed solution to the classical problem of Rayleigh-Bénard convection, with both free and rigid upper and lower boundaries. The computation is facilitated by the use of a newly proposed diagrammatic technique. The resulting equation is a nonlocal pattern equation, which reduces to the 1D Swift-Hohenberg equation for 2D convection. We show that the nonlocal pattern equation is variational by finding a Lyapunov functional.

Subsequently, we formulate a few properties of steady state solutions of general variational PDE, and test their utility in pattern prediction for models including the Swift-Hohenberg equation.

Finally, we describe normal form theory for Hopf bifurcation in the context of pattern equations, and point out possible extensions of the diagrammatic technique.

1 Introduction

In the principal lectures, we learned much about water waves, mostly described by the Korteweg-de Vries (KdV) equation, the nonlinear Schrödinger (NLS) equation, and their generalizations. Both the KdV equation and the NLS equation are Hamiltonian, and thus admit travelling wave solutions with particle-like behavior ("solitons" in the usual sense).

However, if we need to take dissipation (e.g. viscosity, heat diffusivity) and/or forcing (e.g. mechanical vibrations, heat flux) into account, the Hamiltonian structure will likely be destroyed. In hydrodynamics, this happens in the subject of instability [4], within which the Rayleigh-Bénard convection is a prototypical problem.

Near the onset of the Rayleigh-Bénard instability, one can derive an equation for the amplitude of the nearly marginal modes [7]. A systematic procedure (referred to as the Bogoliubov method) for deriving such amplitude equations for a class of instability problems is formulated in [5]. We find that this procedure possesses a mode interaction structure that makes it feasible for expression in terms of Feynman diagrams. Therefore, throughout the derivation we draw these diagrams wherever applicable, and in the end we sketch how this diagrammatic technique can be generalized to other situations, e.g. Hopf bifurcation.

Insofar as the Rayleigh-Bénard convection is concerned, we get a nonlocal equation for the amplitude. We show that this equation possesses a Lyapunov functional $\mathcal{F}$, and thus exhibits features of a gradient dynamical system, namely that the system always evolves towards a local minimum of $\mathcal{F}$. We discover a set of conditions that any solution at a local minimum must satisfy, as long as it is embedded in a zero free-energy background. We

also review the implications of the variational principle for behavior of steady solution near the boundary, as well as a conservation law that follows from Noether's theorem (cf. [12] §9.2.1). We point out that the latter has a natural interpretation in terms of the former.

2   Rayleigh-Bénard Convection

In this section, we formulate in detail the Rayleigh-Bénard convection problem with fixed temperature boundaries.

2.1   Boussinesq Equations

The convection problem is described by the following standard set of non-dimensionalized hydrodynamic equations (cf. [4] II.§7)

$$\partial_t \mathbf{v} + (\mathbf{v} \cdot \nabla)\mathbf{v} + w\partial_z \mathbf{v} = -\nabla\Pi + \varpi(\Delta + \partial_z^2)\mathbf{v}, \tag{1}$$

$$\partial_t w + (\mathbf{v} \cdot \nabla)w + w\partial_z w = -\partial_z\Pi + \varpi(\Delta + \partial_z^2)w + R\varpi\theta, \tag{2}$$

$$\partial_t \theta + (\mathbf{v} \cdot \nabla)\theta + w\partial_z \theta = (\Delta + \partial_z^2)\theta + w, \tag{3}$$

$$\nabla \cdot \mathbf{v} + \partial_z w = 0, \tag{4}$$

where $\nabla = \hat{x}\partial_x + \hat{y}\partial_y$ ($\hat{x}$ and $\hat{y}$ are the two horizontal unit vectors), $\Delta = \nabla^2$, $\mathbf{v}$ is the horizontal velocity, $w\hat{z}$ is the vertical velocity ($\hat{z}$ is the vertical unit vector), and θ and Π are the deviations of the temperature and pressure from their static values. The Prandtl number ϖ and the Rayleigh number R are defined as usual. Typically, we can impose either free or rigid boundary conditions, defined as

$$w = 0, \quad \theta = 0; \quad \partial_z^2 w = 0 \,(\text{free}) \quad \text{or} \quad \partial_z w = 0 \,(\text{rigid}) \quad \text{on} \quad z = \pm\frac{1}{2}. \tag{5}$$

Let us denote the full velocity as $\mathbf{u} = (\mathbf{v}, w)$, and the full vorticity as $\boldsymbol{\omega} = \nabla \times \mathbf{u}$, where $\nabla = \hat{x}\partial_x + \hat{y}\partial_y + \hat{z}\partial_z$. The full vorticity equation is then (cf. [13] §5.5)

$$\frac{D\boldsymbol{\omega}}{Dt} = (\boldsymbol{\omega} \cdot \nabla)\mathbf{u} + \varpi\nabla^2\boldsymbol{\omega} + \nabla \times (R\varpi\theta\hat{z}). \tag{6}$$

From (5), we get the following boundary conditions on the vertical vorticity $\zeta \equiv (\nabla \times \mathbf{v}) \cdot \hat{z}$

$$\partial_z\zeta = 0 \,(\text{free}) \quad \text{or} \quad \zeta = 0 \,(\text{rigid}) \quad \text{on} \quad z = \pm\frac{1}{2}. \tag{7}$$

The significance of ζ is that, given w and ζ, we can uniquely determine $\mathbf{v}$ up to a gauge using the relations $\nabla \cdot \mathbf{v} = -\partial_z w$, $\nabla \times \mathbf{v} = \zeta\hat{z}$. Therefore, (ζ, w, θ) provides a complete description of the state of the fluid. Now we formulate linear theory based on this set of variables.

2.2   Linear Theory

Taking the $\hat{z}$-component of (6) and linearizing, we get an uncoupled equation for ζ

$$\partial_t\zeta = \varpi\nabla^2\zeta.$$

In view of (7), if we take the boundaries at $z = \pm 1/2$ both to be rigid surfaces, then all the vertical vorticity modes are strongly damped. However, for two free boundaries, there is a solution with ζ constant in space and time corresponding to a rigid, undamped rotation of the whole fluid. In a finite system, such modes of motion play no role, and the only motions consisting of purely vertical vorticity are viscously damped. These will be slave modes, in the jargon of dynamical systems theory. Hence we shall not allow for their nonlinear excitation here and so make the approximation

$$\zeta = 0 \quad \text{for all} \quad t. \tag{8}$$

The case of one rigid and one free boundary is mathematically similar to two rigid boundaries. The case of nonzero ζ is studied in [17] and [21].

Now the fields w and θ completely specify the state of the fluid. To write the Boussinesq equations only in terms of w and θ, we shall keep (3) but for (1) and (2), we need to eliminate Π by $-\partial_z \nabla \cdot (1) + \Delta(2)$. The linear parts of these two equations are

$$\partial_t (\partial_z^2 + \Delta)w = \varpi(\partial_z^2 + \Delta)^2 w + R\varpi\Delta\theta, \quad \partial_t\theta = w + (\partial_z^2 + \Delta)\theta. \tag{9}$$

It is thus convenient to work in the Fourier space with

$$\Diamond(\mathbf{x}, z, t) = \int \Diamond_{\mathbf{k}}(z, t)e^{i\mathbf{k}\cdot\mathbf{x}}d\mathbf{k},$$

where $\Diamond = w$, θ or $\mathbf{v}$. We may define $\mathbf{U_k} \equiv (w_{\mathbf{k}}, \theta_{\mathbf{k}})^T$ and write (9) succinctly as

$$\partial_t \mathbb{M}_{\mathbf{k}} \mathbf{U_k} = \mathbb{L}_{\mathbf{k}} \mathbf{U_k}, \tag{10}$$

where

$$\mathbb{M}_{\mathbf{k}} = \begin{pmatrix} \partial_z^2 - \mathbf{k}^2 & 0 \\ 0 & 1 \end{pmatrix}, \quad \mathbb{L}_{\mathbf{k}} = \begin{pmatrix} \varpi\left(\partial_z^2 - \mathbf{k}^2\right)^2 & -\mathbf{k}^2 R\varpi \\ 1 & \partial_z^2 - \mathbf{k}^2 \end{pmatrix}, \tag{11}$$

and the boundary conditions follow from (5)

$$\mathbf{U_k} = \mathbf{0}, \quad (1,0)\partial_z^2\mathbf{U_k} = 0 \,(\text{free}) \quad \text{or} \quad (1,0)\partial_z\mathbf{U_k} = 0 \,(\text{rigid}) \quad \text{on} \quad z = \pm\frac{1}{2}. \tag{12}$$

This linear problem is separable, and we may seek solutions of the form $\Phi_{\mathbf{k}}(z)e^{st}$. For either free or rigid boundaries, there is a pair of $\Phi_{\mathbf{k}}(z)$ with l nodes for each $l = 0, 1, 2, \cdots$. One lowest vertical mode, denoted by $\phi_{\mathbf{k}}(z)$, can go unstable with growth rate denoted by $\sigma_{\mathbf{k}}$. The other lowest vertical mode, denoted by $\varphi_{\mathbf{k}}(z)$, and the higher vertical modes, denoted by $\chi_{\mathbf{k},l}^{\pm}(z)$ $(l = 1, 2, \cdots)$, are always stable with growth rate denoted by $\tau_{\mathbf{k}}$ and $\omega_{\mathbf{k},l}^{\pm}$. The functions $\phi_{\mathbf{k}}$, $\varphi_{\mathbf{k}}$ and $\chi_{\mathbf{k},l}^{\pm}$ form an orthogonal basis with the inner product

$$\langle \mathbf{U_k}, \tilde{\mathbf{U}}_{\mathbf{k}} \rangle \equiv \int_{-\frac{1}{2}}^{\frac{1}{2}} \left(w_{\mathbf{k}}^*(\mathbf{k}^2 - \partial_z^2)\tilde{w}_{\mathbf{k}} + R\varpi\theta_{\mathbf{k}}^*\mathbf{k}^2\tilde{\theta}_{\mathbf{k}} \right) dz,$$

where * denotes complex conjugate.

It follows from (10) that the linear problems for $\phi_{\mathbf{k}}$, and its adjoint $\phi_{\mathbf{k}}^{\dagger}$, are

$$\mathbb{L}_{\mathbf{k}}\phi_{\mathbf{k}} = \sigma_{\mathbf{k}}\mathbb{M}_{\mathbf{k}}\phi_{\mathbf{k}}, \quad \mathbb{L}_{\mathbf{k}}^{\dagger}\phi_{\mathbf{k}}^{\dagger} = \sigma_{\mathbf{k}}\mathbb{M}_{\mathbf{k}}^{\dagger}\phi_{\mathbf{k}}^{\dagger},$$

where the adjoint operators are the transposes of the original ones, and the adjoint boundary conditions coincide with the original ones ($\sigma_\mathbf{k}$ can be shown to be real for our range of R).

The critical point is $(R_c, k_c) = (27\pi^4/4, \pi/\sqrt{2})$ for free boundaries, and $(R_c, k_c) = (1708, 3.116)$ for rigid boundaries (cf. [4] II.§15(b)). For (R, k) near (R_c, k_c), we have the expansion [7] for free boundaries

$$\sigma_k = \frac{k_c^2 \varpi}{\varpi + 1} \left(3(\frac{R}{R_c} - 1) - \frac{(k^2 - k_c^2)^2}{k_c^4} \right), \tag{13}$$

and for rigid boundaries

$$\sigma_k = \frac{19.65\varpi}{\varpi + 0.5117} \left((\frac{R}{R_c} - 1) - 0.3593\frac{(k^2 - k_c^2)^2}{k_c^4} \right). \tag{14}$$

The solution at (R_c, k_c) and its adjoint are, for free boundaries

$$\phi_{k_c}(z) = \hat{\phi}_{k_c} \cos(\pi z), \quad \hat{\phi}_{k_c} = \begin{pmatrix} 1 \\ 1/(3k_c^2) \end{pmatrix};$$

$$\phi_{k_c}^\dagger(z) = \hat{\phi}_{k_c}^\dagger \cos(\pi z), \quad \hat{\phi}_{k_c}^\dagger = \begin{pmatrix} 1 \\ -9k_c^4\varpi \end{pmatrix}.$$

For rigid boundaries

$$\phi_{k_c}(z) = \begin{pmatrix} W_{k_c}(z) \\ (k_c^2 R)^{-1/3}\Theta_{k_c}(z) \end{pmatrix}, \quad \phi_{k_c}^\dagger(z) = \begin{pmatrix} W_{k_c}(z) \\ -\varpi (k_c^2 R)^{2/3}\Theta_{k_c}(z) \end{pmatrix},$$

where the functions W_{k_c} and Θ_{k_c} are defined by

$$\begin{aligned} W_{k_c}(z) &= \cos q_0 z + (A_1 + iA_2)\cos i(q_1 + iq_2)z + (A_1 - iA_2)\cos i(q_1 - iq_2)z, \\ \Theta_{k_c}(z) &= \cos q_0 z + (B_1 + iB_2)\cos i(q_1 + iq_2)z + (B_1 - iB_2)\cos i(q_1 - iq_2)z, \end{aligned}$$

with $q_0 = 3.974$, $q_1 = 5.194$, $q_2 = 2.126$, $A_1 = -0.03076$, $A_2 = -0.05196$, $B_1 = 0.06038$ and $B_2 = -0.0006647$.

2.3 Nonlinear Terms

In the Fourier space, $\mathbf{v_k}$ can be expressed in terms of $w_\mathbf{k}$, by (4) and (8), as

$$\mathbf{v_k} = \frac{i\mathbf{k}}{\mathbf{k}^2}\partial_z w_\mathbf{k}. \tag{15}$$

With this, we can work out the nonlinear terms in (1-4). First, we transform (3) into the form

$$\partial_t \theta_\mathbf{k} = w_\mathbf{k} + (\partial_z^2 - \mathbf{k}^2)\theta_\mathbf{k} + \iint \mathcal{N}_\theta \delta(\mathbf{k} - \mathbf{p} - \mathbf{q})d\mathbf{p}d\mathbf{q}. \tag{16}$$

To determine the nonlinear part $\mathcal{N}_\theta$, we note that $-w\partial_z\theta$ yields $-w_\mathbf{q}\partial_z\theta_\mathbf{p}$, and $-(\mathbf{v} \cdot \nabla)\theta$ yields

$$-(\mathbf{v} \cdot \nabla)\theta = -\int (i\mathbf{v} \cdot \mathbf{p})\theta_\mathbf{p}e^{i\mathbf{p}\cdot\mathbf{x}}d\mathbf{p},$$

311

where, by (15)

$$-(i\mathbf{v} \cdot \mathbf{p}) = \int \frac{\mathbf{p} \cdot \mathbf{q}}{\mathbf{q}^2} \partial_z w_{\mathbf{q}} e^{i\mathbf{q} \cdot \mathbf{x}} d\mathbf{q}.$$

We then obtain

$$\mathcal{N}_\theta = \frac{\mathbf{p} \cdot \mathbf{q}}{\mathbf{q}^2} \theta_{\mathbf{p}} \partial_z w_{\mathbf{q}} - w_{\mathbf{q}} \partial_z \theta_{\mathbf{p}}. \tag{17}$$

As for (1) and (2), let us recall that we need to first eliminate Π by $-\partial_z \nabla \cdot (1) + \Delta(2)$. The resulting equation has four nonlinear terms on the right

$$(A)\partial_z \nabla \cdot ((\mathbf{v} \cdot \nabla)\mathbf{v}); (B)\partial_z \nabla \cdot (w\partial_z \mathbf{v}); (C) - \Delta((\mathbf{v} \cdot \nabla)w); (D) - \Delta(w\partial_z w). \tag{18}$$

The incarnation of this equation in the Fourier space is

$$\partial_t(\partial_z^2 - \mathbf{k}^2)w_{\mathbf{k}} = \varpi(\partial_z^2 - \mathbf{k}^2)^2 w_{\mathbf{k}} - \mathbf{k}^2 R\varpi \theta_{\mathbf{k}} + \iint \mathcal{N}_w \delta(\mathbf{k} - \mathbf{p} - \mathbf{q}) d\mathbf{p} d\mathbf{q}. \tag{19}$$

The contributions of (18) to $\mathcal{N}_w$ can be worked out by switching to index notation, doing the Fourier transform, and finally returning to vector notation. The results are

$$(A)(\frac{(\mathbf{p} \cdot \mathbf{q})^2}{\mathbf{p}^2 \mathbf{q}^2} + \frac{\mathbf{p} \cdot \mathbf{q}}{\mathbf{p}^2})\partial_z(\partial_z w_{\mathbf{p}} \partial_z w_{\mathbf{q}}); \qquad (B) - (\frac{\mathbf{p} \cdot \mathbf{q}}{\mathbf{q}^2} + 1)\partial_z(w_{\mathbf{p}} \partial_z^2 w_{\mathbf{q}});$$

$$(C) - (\mathbf{p} \cdot \mathbf{q} + 2\frac{(\mathbf{p} \cdot \mathbf{q})^2}{\mathbf{p}^2} + \frac{\mathbf{q}^2}{\mathbf{p}^2}\mathbf{p} \cdot \mathbf{q})w_{\mathbf{q}} \partial_z w_{\mathbf{p}}; \qquad (D)(\mathbf{p}^2 + 2\mathbf{p} \cdot \mathbf{q} + \mathbf{q}^2)w_{\mathbf{p}} \partial_z w_{\mathbf{q}}.$$

To simplify the expression, we can exchange $\mathbf{p}$ and $\mathbf{q}$ in any term. The overall sum is

$$\begin{aligned}
\mathcal{N}_w &= (2\frac{(\mathbf{p} \cdot \mathbf{q})^2}{\mathbf{p}^2 \mathbf{q}^2} + \frac{\mathbf{p} \cdot \mathbf{q}}{\mathbf{p}^2} - 1)\partial_z w_{\mathbf{p}} \partial_z^2 w_{\mathbf{q}} - (\frac{\mathbf{p} \cdot \mathbf{q}}{\mathbf{q}^2} + 1)w_{\mathbf{p}} \partial_z^3 w_{\mathbf{q}} \\
&\quad -(2\frac{(\mathbf{p} \cdot \mathbf{q})^2}{\mathbf{q}^2} + (\frac{\mathbf{p}^2}{\mathbf{q}^2} - 1)\mathbf{p} \cdot \mathbf{q} - \mathbf{p}^2 - \mathbf{q}^2)w_{\mathbf{p}} \partial_z w_{\mathbf{q}}. \tag{20}
\end{aligned}$$

In terms of $\mathbf{U_k} \equiv (w_{\mathbf{k}}, \theta_{\mathbf{k}})^T$, we may write (16) and (19) succinctly as

$$\partial_t \mathbb{M}_{\mathbf{k}} \mathbf{U_k} = \mathbb{L}_{\mathbf{k}} \mathbf{U_k} + \iint \mathcal{N} \delta(\mathbf{k} - \mathbf{p} - \mathbf{q}) d\mathbf{p} d\mathbf{q}, \tag{21}$$

where $\mathcal{N} \equiv (\mathcal{N}_w, \mathcal{N}_\theta)^T$, and the boundary conditions are given in (12).

3   The Expansion Procedure

In this section, we follow [5] §6 to employ the Bogoliubov approach to derive the pattern equation for the convection problem. Note that the results differ from [5] in some details.

3.1 The Diagrammatic Notation

We can express (21) diagrammatically, with the replacement $\mathbf{U} \to \circ$, as

$$\partial_t \circ\!\!-\!\!-\mathbb{M} \;=\; \circ\!\!-\!\!-\mathbb{L} \;+\; {\LARGE>}\mathcal{N} \,.$$

This type of diagram, regarded for now simply as a device to keep track of terms in perturbation series, bears some resemblance to Feynman diagrams in quantum field theory. The lines carry momenta, or wave vectors, although these are typically not labelled. The vertices conserve momenta, as reflected by the δ-function of wave vectors. Each diagram corresponds to a unique term in the perturbation series. At any given order, one first draws all possible (Feynman) diagrams consistent with certain physical laws, and then translates these diagrams back to algebraic expressions with a prescribed set of Feynman rules. As Feynman diagrams are frequently used in particle physics [16], condensed matter physics [15] as well as the theories of turbulence in fluids [25] and wave propagation in random media [10], we hope that their use here will simplify the calculation of modal interactions in convection.

The diagrams are largely self-explanatory except for a few conventions. All the symbols in the diagrams are vertices except for the special operator ∂_t. For any vertex, the lines immediately to its left (right) are called incoming (outgoing) lines, and the number of incoming (outgoing) lines is called the indegree (outdegree) of that vertex. We observe that all the vertices have outdegree one, but the indegree can be one (e.g. $\mathbb{M}$, $\mathbb{L}$) or more (e.g. $\mathcal{N}$). If only such vertices are present, the diagram necessarily takes the form of a tree, consisting of the *root* connected to the *leaves* via the *stems*. These diagrams differ from those in quantum field theory, where particles can be either created or annihilated, thereby making loops possible. Note that the leftmost incoming line(s) entering the leaves and the rightmost outgoing line exiting the root are not shown explicitly. The total number of leaves is the order of the diagram, consistent with perturbation theory practice.

How to translate a diagram back to an algebraic expression? The case of a first order diagram is obvious. For an n-th order diagram ($n \geq 2$), we first label the wave vectors entering the leaves as, say, $\mathbf{p}_1, \cdots, \mathbf{p}_n$, and the wave vector exiting the root as, say, $\mathbf{k}$. Then we label the wave vectors on the stems in terms of $\mathbf{p}_1, \cdots, \mathbf{p}_n$, using conservation of wave wave vectors at the vertices. Any vertex corresponds to a function the wave vectors on its incoming lines and the sub-diagrams connected to it through these lines ($\mathcal{N}$ is a somehow complicated example). With these guidelines, for any tree diagram, we can start from its root, traverse its stems and finally reach its leaves. The expression that we get, multiplied by $\delta(\mathbf{k} - \mathbf{p}_1 - \cdots - \mathbf{p}_n)$ and integrated over $\mathbf{p}_1, \cdots, \mathbf{p}_n$, is the final result. We remark that the wave wave vectors carried by the intermediate stems are automatically integrated out, so only the δ-function describing the overall wave vector conservation remains.

Now things are ready for deriving the amplitude equation. For this purpose, we need to eliminate the fast modes and keep the slow modes, much like the process of center manifold reduction in bifurcation theory for ODE. However, in generalizing the procedure to PDE, we encounter an inherent difficulty. Before dealing with the convection problem, we explain the reduction procedure with an illustrative example, where this difficulty clearly figures.

3.2 Irremovable Resonances

To illustrate the procedure we consider the following equations [24] whose structures are reminiscent of (21)

$$\partial_t f_{\mathbf{k}} = \sigma_{\mathbf{k}} f_{\mathbf{k}} + \iint f_{\mathbf{p}} g_{\mathbf{q}} \delta(\mathbf{k} - \mathbf{p} - \mathbf{q}) d\mathbf{p} d\mathbf{q},$$

$$\partial_t g_{\mathbf{k}} = \gamma_{\mathbf{k}} g_{\mathbf{k}} + \iint f_{\mathbf{p}} f_{\mathbf{q}} \delta(\mathbf{k} - \mathbf{p} - \mathbf{q}) d\mathbf{p} d\mathbf{q},$$

which, with the replacements $f \to \circ$, $g \to \circ$, can be represented diagrammatically as

$$\partial_t \circ \; = \; \circ\!\!-\!\!-\!\!\sigma \; + \; \rangle\!\mathcal{N} \, , \tag{22}$$

$$\partial_t \circ \; = \; \circ\!\!-\!\!-\!\!\gamma \; + \; \rangle\!\mathcal{N} \, , \tag{23}$$

where $\sigma_{\mathbf{k}} = \sigma - (k^2 + k_1^2)^2$ and $\gamma_{\mathbf{k}} = \gamma - (k^2 + k_2^2)^2$ with $\gamma < 0$ and $|\sigma| \ll |\gamma|$. The vertex $\mathcal{N}$ here simply takes the product of the two sub-diagrams connected to it.

We seek a near-identity coordinate change (here $F_{\mathbf{k}}$ is the coordinate on the "center manifold")

$$f_{\mathbf{k}} = F_{\mathbf{k}} + \iint \mathcal{I}_{\mathbf{k}}(\mathbf{p}, \mathbf{q}) F_{\mathbf{p}} F_{\mathbf{q}} d\mathbf{p} d\mathbf{q} + \cdots ,$$

$$g_{\mathbf{k}} = G_{\mathbf{k}} + \iint \mathcal{J}_{\mathbf{k}}(\mathbf{p}, \mathbf{q}) F_{\mathbf{p}} F_{\mathbf{q}} d\mathbf{p} d\mathbf{q} + \cdots ,$$

represented diagrammatically, with $F \to \bullet$, $G \to \bullet$, as

$$\circ \; = \; \bullet \; + \; \rangle\!\mathcal{I} \; + \cdots , \tag{24}$$

$$\circ \; = \; \bullet \; + \; \rangle\!\mathcal{J} \; + \cdots , \tag{25}$$

which turns (22-23) into the standard form

$$\partial_t F_{\mathbf{k}} = \sigma_{\mathbf{k}} F_{\mathbf{k}} + \iint \Phi_{\mathbf{k}}(\mathbf{p}, \mathbf{q}) F_{\mathbf{p}} F_{\mathbf{q}} d\mathbf{p} d\mathbf{q} + \cdots ,$$

$$\partial_t G_{\mathbf{k}} = \left(\gamma_{\mathbf{k}} + \int \Psi_{\mathbf{k}}(\mathbf{p}) F_{\mathbf{p}} d\mathbf{p} + \cdots \right) G_{\mathbf{k}} + \cdots ,$$

represented diagrammatically as

$$\partial_t \bullet \; = \; \bullet\!\!-\!\!-\!\!\sigma \; + \; \rangle\!\Phi \; + \cdots , \tag{26}$$

$$\partial_t \bullet \; = \; (\gamma + \; \bullet\!\!-\!\!-\!\!\Psi \; + \cdots)\!\!-\!\!-\!\!\bullet \; + \cdots . \tag{27}$$

In order that (24-25) produce (27) from (23) (or equivalently, a functional analogue of a center manifold exists in a loose sense), we must satisfy, at second order

$$2 \; \bullet\!\rangle^{\sigma}\!\mathcal{J} \; = \; \bullet\!\rangle_{\mathcal{J}}\!\!-\!\!\gamma \; + \; \bullet\!\rangle\!\mathcal{N} \, . \tag{28}$$

Two points should be noted in the interpretation of the first diagram. First, the factor of 2, known as the symmetry factor in quantum field theory, refers to the two distinct
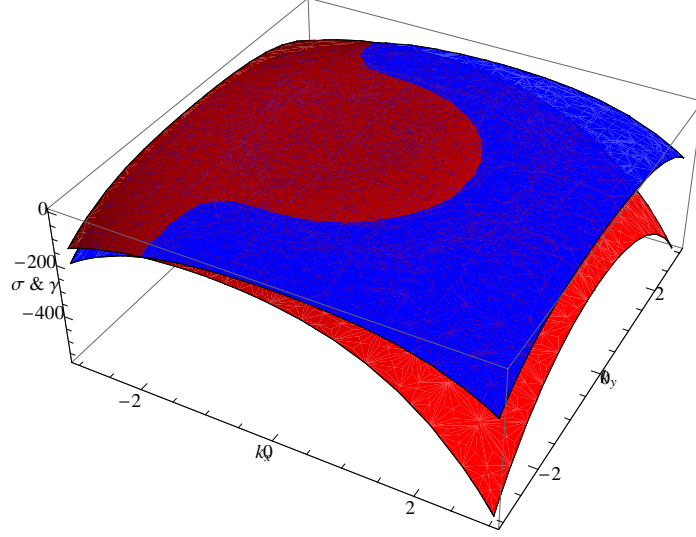
Figure 1: The curve of resonances. We plot $\sigma + \sigma_{\mathbf{k}+k_1\hat{x}}$ in red and $\gamma_{\mathbf{k}}$ in blue, with their intersection implying resonances. Parameters: $k_1 = 1$, $k_2 = 2$, $\sigma = 0.1$, $\gamma = -5$.

ways to permutate the incoming edges of $\mathcal{J}$. Graphically these two permutations can be combined, but algebraically they represent two different terms involving the two arguments of $\mathcal{J}$. Second, the vertex σ has indegree and outdegree both one, so it simply propagates the wave vector through itself. At any such vertex, the line is deliberately bent to signify the presence of the vertex. In contrast, for a vertex with indegree two (or more) and outdegree one (e.g. $\mathcal{J}$), its presence is already apparent from the topology of the diagram.

It follows that (28) translates to the condition

$$\iint \left(\mathcal{D}_{\mathbf{k}}(\mathbf{p},\mathbf{q})\mathcal{J}_{\mathbf{k}}(\mathbf{p},\mathbf{q}) - \delta(\mathbf{p}+\mathbf{q}-\mathbf{k})\right) F_{\mathbf{p}}F_{\mathbf{q}}d\mathbf{p}d\mathbf{q} = 0, \tag{29}$$

where $\mathcal{D}_{\mathbf{k}}(\mathbf{p},\mathbf{q}) = \sigma_{\mathbf{p}} + \sigma_{\mathbf{q}} - \gamma_{\mathbf{k}}$. There are resonances when

$$\mathbf{p} + \mathbf{q} - \mathbf{k} = 0, \quad \mathcal{D}_{\mathbf{k}}(\mathbf{p},\mathbf{q}) = 0.$$

These resonances cannot occur if both $|\mathbf{p}|$ and $|\mathbf{q}|$ are near k_1, but they do occur when we take, say, only $\mathbf{p} = k_1\hat{x}$. We can find the curve of resonances (Fig. 1) with the graphical procedure (cf. [2], [27]) mentioned in Lecture 12 – Triad Resonances.

It is an open question whether these resonances are artifacts of the procedure, although there is evidence that they indeed are [24].

To get the pattern equation, we introduce (25) into (22). On the center manifold, by definition, $\bullet = 0$. In addition, we have the freedom to identify $\circ$ with $\bullet$. Therefore, the pattern equation truncated to third order is

$$\partial_t \bullet \;=\; \bullet \!\!-\!\!-\!\!-\!\! \sigma \;+\; \bullet \!\!\!\genfrac{}{}{0pt}{}{}{}\!\!\!\!\!\!\mathcal{N} \;, \tag{30}$$

which translates to

$$\partial_t F_{\mathbf{k}} = \sigma_{\mathbf{k}} F_{\mathbf{k}} + \iiint \mathcal{J}(\mathbf{q},\mathbf{r})\delta(\mathbf{k}-\mathbf{p}-\mathbf{q}-\mathbf{r})F_{\mathbf{p}}F_{\mathbf{q}}F_{\mathbf{r}}d\mathbf{p}d\mathbf{q}d\mathbf{r},$$

where $\mathcal{J}$ is determined from (29) by the method of steepest descent [24].

3.3 Nonlinear Expansions

Now we attempt to apply center manifold reduction to the Boussinesq convection problem. A crucial observation is that once we admit that an effective (or functional) center manifold exists, all physical quantities depend only on the amplitudes of the slow modes. This is the spirit of the Bogoliubov method that we use.

Since the growth rate $\sigma_{\mathbf{k}}$ depends continuously on $\mathbf{k}$, one needs to introduce a cutoff in $\mathbf{k}$ to define which modes are slow. We will choose the cutoff for computational convenience, but point out that no choice is truly justified due to the lack of spectral gap.

3.3.1 Setup

The key idea is the expressibility of $\mathbf{U_k}$ as the functional power series

$$\mathbf{U_k} = A_{\mathbf{k}}\phi_{\mathbf{k}} + \iint d\mathbf{p}d\mathbf{q}A_{\mathbf{p}}A_{\mathbf{q}}\mathcal{U}_{\mathbf{k}}^{(2)}(\mathbf{p},\mathbf{q};z) + \cdots, \tag{31}$$

where $A_{\mathbf{k}}$ satisfies

$$\partial_t A_{\mathbf{k}} = \sigma_k A_{\mathbf{k}} + \iint d\mathbf{p}d\mathbf{q}A_{\mathbf{p}}A_{\mathbf{q}}\Gamma_{\mathbf{k}}^{(2)}(\mathbf{p},\mathbf{q}) + \cdots. \tag{32}$$

We can express (31) and (32) diagrammatically with $A \to \bullet$ as

We substitute into (21) and gather terms of the same order in $A_{\mathbf{k}}$. The linear condition

is satisfied for a suitable choice of $\phi_{\mathbf{k}}$. At each higher order, the kernel must cancel out because $A_{\mathbf{k}}$ is arbitrary. Let $\mathcal{N}^{(m)}$ denote the coefficient of the δ-function in the kernel of $\mathcal{N}$ at the m-th order. To approximate, we take $A_{\mathbf{k}}$ to have *infinitesimal support* around the critical circle $|\mathbf{k}| = k_c$. Therefore, we can set the corresponding growth rate $\sigma_{\mathbf{k}} = 0$.

3.3.2 Second order

Setting the kernel of the gathered second order terms to 0, we get

$$-\mathbb{L}_{\mathbf{k}}\mathcal{U}_{\mathbf{k}}^{(2)} = \mathcal{N}^{(2)}(\mathbf{p},\mathbf{q})\delta(\mathbf{k}-\mathbf{p}-\mathbf{q}) - \Gamma_{\mathbf{k}}^{(2)}(\mathbf{p},\mathbf{q})\mathbb{M}_{\mathbf{k}}\phi_{\mathbf{k}}.$$
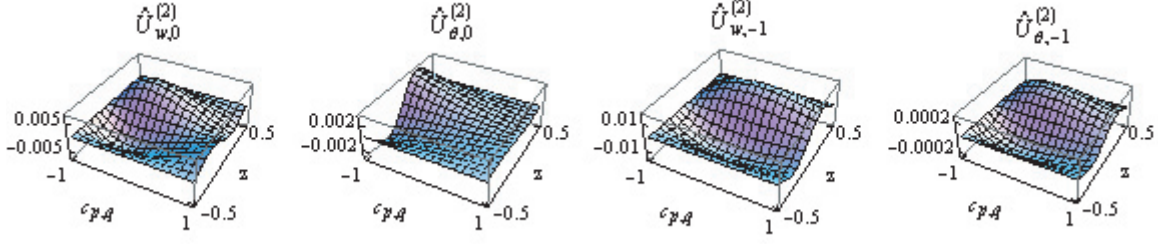
Figure 2: Plot of $\hat{\mathcal{U}}_{w,0}^{(2)}$, $\hat{\mathcal{U}}_{\theta,0}^{(2)}$, $\hat{\mathcal{U}}_{w,-1}^{(2)}$ and $\hat{\mathcal{U}}_{\theta,-1}^{(2)}$ as functions of z and $c_{\mathbf{p},\mathbf{q}}$.

The solvability condition ($\mathcal{N}^{(2)}$ being odd does not contain the lowest vertical mode)

$$0 = -\Gamma_{\mathbf{k}}^{(2)}(\mathbf{p},\mathbf{q})\langle(\phi_{\mathbf{k}}^{\dagger})^{T}|\mathbb{M}_{\mathbf{k}}\phi_{\mathbf{k}}\rangle$$

determines that $\Gamma_{\mathbf{k}}^{(2)}(\mathbf{p},\mathbf{q}) = 0$. Here $\langle\cdot|\cdot\rangle$ denotes the usual inner product. We are left with an always solvable equation

$$-\mathbb{L}_{\mathbf{k}}\mathcal{U}_{\mathbf{k}}^{(2)} = \mathcal{N}^{(2)}(\mathbf{p},\mathbf{q})\delta(\mathbf{k}-\mathbf{p}-\mathbf{q}).$$

Here, $\mathbf{p}$ and $\mathbf{q}$ are constrained to lie on the critical circle but $\mathbf{k}$ is not. If we introduce the shorthand $c_{\mathbf{p},\mathbf{q}} \equiv \mathbf{p}\cdot\mathbf{q}/\sqrt{\mathbf{p}^2\mathbf{q}^2}$, then

$$\mathcal{N}_\theta = c_{\mathbf{p},\mathbf{q}}\theta_{\mathbf{p}}\partial_z w_{\mathbf{q}} - w_{\mathbf{q}}\partial_z\theta_{\mathbf{p}},$$
$$\mathcal{N}_w = (2c_{\mathbf{p},\mathbf{q}}^2 + c_{\mathbf{p},\mathbf{q}} - 1)\partial_z w_{\mathbf{p}}\partial_z^2 w_{\mathbf{q}} - (c_{\mathbf{p},\mathbf{q}} + 1)w_{\mathbf{p}}\partial_z^3 w_{\mathbf{q}} - 2k_c^2(c_{\mathbf{p},\mathbf{q}}^2 - 1)w_{\mathbf{p}}\partial_z w_{\mathbf{q}}.$$

The matrix $\mathbb{L}_{\mathbf{k}} = \mathbb{L}_{\mathbf{p}+\mathbf{q}}$ also depends on $c_{\mathbf{p},\mathbf{q}}$. These lead to

$$\mathcal{U}_{\mathbf{k}}^{(2)}(\mathbf{p},\mathbf{q};z) = \hat{\mathcal{U}}^{(2)}(\varpi,z,c_{\mathbf{p},\mathbf{q}})\delta(\mathbf{k}-\mathbf{p}-\mathbf{q}).$$

For free boundaries, we have the relatively simple expression

$$\hat{\mathcal{U}}^{(2)}(\varpi,z,c_{\mathbf{p},\mathbf{q}}) = \frac{1-c_{\mathbf{p},\mathbf{q}}}{(5+c_{\mathbf{p},\mathbf{q}})^3 - \frac{27}{4}(1+c_{\mathbf{p},\mathbf{q}})}\left(\begin{array}{c}\frac{3(1+c_{\mathbf{p},\mathbf{q}})(3+2(5+c_{\mathbf{p},\mathbf{q}})\varpi^{-1})}{4\pi}\\\frac{2(5+c_{\mathbf{p},\mathbf{q}})^2+9(1+c_{\mathbf{p},\mathbf{q}})\varpi^{-1}}{6\pi^3}\end{array}\right)\sin(2\pi z).$$

For rigid boundaries, it turns out easier to evaluate $\hat{\mathcal{U}}^{(2)}$ numerically rather than analytically. The result can be written as

$$\hat{\mathcal{U}}^{(2)}(\varpi,z,c_{\mathbf{p},\mathbf{q}}) = \left(\begin{array}{c}\hat{\mathcal{U}}_{w,0}^{(2)}(z,c_{\mathbf{p},\mathbf{q}})\\\hat{\mathcal{U}}_{\theta,0}^{(2)}(z,c_{\mathbf{p},\mathbf{q}})\end{array}\right) + \left(\begin{array}{c}\hat{\mathcal{U}}_{w,-1}^{(2)}(z,c_{\mathbf{p},\mathbf{q}})\\\hat{\mathcal{U}}_{\theta,-1}^{(2)}(z,c_{\mathbf{p},\mathbf{q}})\end{array}\right)\varpi^{-1},$$

where the functions $\hat{\mathcal{U}}_{w,0}^{(2)}$, $\hat{\mathcal{U}}_{\theta,0}^{(2)}$, $\hat{\mathcal{U}}_{w,-1}^{(2)}$ and $\hat{\mathcal{U}}_{\theta,-1}^{(2)}$ are plotted in Fig. 2.

3.3.3 Third order

$$\text{(diagram)} \quad + 2 \; \text{(diagram)} \;\mathbb{M} \;=\; \text{(diagram)} \;\mathbb{L} \;+\; 2\; \text{(diagram)}\;\mathcal{N}\;.$$

Setting the kernel of the gathered third order terms to 0, we get

$$-\mathbb{L}_{\mathbf{k}}\mathcal{U}_{\mathbf{k}}^{(3)} = \mathcal{N}^{(3)}(\mathbf{p},\mathbf{q},\mathbf{r})\delta(\mathbf{k}-\mathbf{p}-\mathbf{q}-\mathbf{r}) - \Gamma_{\mathbf{k}}^{(3)}(\mathbf{p},\mathbf{q},\mathbf{r})\mathbb{M}_{\mathbf{k}}\phi_{\mathbf{k}}.$$

Because $\mathbf{k}$, $\mathbf{p}$, $\mathbf{q}$ and $\mathbf{r}$ are all restricted to the critical circle, we have only three possibilities

$$\text{(I)}\,\mathbf{k}=\mathbf{p},\,\mathbf{q}=-\mathbf{r}; \quad \text{(II)}\,\mathbf{k}=\mathbf{q},\,\mathbf{r}=-\mathbf{p}; \quad \text{(III)}\,\mathbf{k}=\mathbf{r},\,\mathbf{p}=-\mathbf{q}. \tag{33}$$

Now we let $\mathbf{p}$ (resp. $\mathbf{q}$ and $\mathbf{r}$) denote the wave vector(s) in the first (resp. second) order. If we suitably permutate $\mathbf{p}$, $\mathbf{q}$ and $\mathbf{r}$, we can transform all three cases to the geometry of case (II). Thus the contribution from case (III) is identical to case (II), but differs from case (I). We find, with some algebra, that

$$\mathcal{N}^{(3)} = 2\left(\begin{array}{c}\hat{\mathcal{U}}_w\left(k_c^2\left(2+c_{q,r}\right)\phi_w' + c_{q,r}\phi_w{}^{(3)}\right) + \frac{1}{2}\cdot \\ \cdot\left(\left(3k_c^2\phi_w + (-1+2c_{q,r})\phi_w''\right)\hat{\mathcal{U}}_w{}^{(0,1,0)} - 2\phi_w'\hat{\mathcal{U}}_w{}^{(0,2,0)} - \phi_w\hat{\mathcal{U}}_w{}^{(0,3,0)}\right) \\ \frac{1}{2}\left(-2\hat{\mathcal{U}}_\theta\left(1+c_{q,r}\right)\phi_w' - 2\hat{\mathcal{U}}_w\phi_\theta' - \phi_\theta\hat{\mathcal{U}}_w{}^{(0,1,0)} - 2\phi_w\hat{\mathcal{U}}_\theta{}^{(0,1,0)}\right)\end{array}\right) + \mathcal{N}_{(\text{I})}^{(3)},$$

where subscript (I) denotes case (I). The following solvability condition must be satisfied

$$\langle(\phi_{\mathbf{k}}^\dagger)^T|\mathcal{N}^{(3)}(\mathbf{p},\mathbf{q},\mathbf{r})\delta(\mathbf{k}-\mathbf{p}-\mathbf{q}-\mathbf{r}) - \Gamma_{\mathbf{k}}^{(3)}(\mathbf{p},\mathbf{q},\mathbf{r})\mathbb{M}_{\mathbf{k}}\phi_{\mathbf{k}}\rangle = 0.$$

For either free or rigid boundaries, we have the general expression

$$\Gamma_{\mathbf{k}}^{(3)}(\mathbf{p},\mathbf{q},\mathbf{r}) = \hat{\Gamma}^{(3)}(\varpi,c_{\mathbf{q},\mathbf{r}})\delta(\mathbf{k}-\mathbf{p}-\mathbf{q}-\mathbf{r}). \tag{34}$$

In the free case, we have the relatively simple expression

$$\hat{\Gamma}^{(3)}(\varpi,c_{\mathbf{q},\mathbf{r}}) = 2\hat{\Gamma}_{(\text{II})}^{(3)} + \hat{\Gamma}_{(\text{I})}^{(3)} \tag{35}$$

where

$$\hat{\Gamma}_{(\text{II})}^{(3)} = -\frac{\varpi}{4(1+\varpi)}\frac{(1-c_{\mathbf{q},\mathbf{r}})^2((5+c_{\mathbf{q},\mathbf{r}})^2 + 9(1+c_{\mathbf{q},\mathbf{r}})\varpi^{-1} + 3(1+c_{\mathbf{q},\mathbf{r}})(5+c_{\mathbf{q},\mathbf{r}})\varpi^{-2})}{(5+c_{\mathbf{q},\mathbf{r}})^3 - \frac{27}{4}(1+c_{\mathbf{q},\mathbf{r}})}$$

and

$$\hat{\Gamma}_{(\text{I})}^{(3)} = -\frac{\varpi}{4(1+\varpi)}. \tag{36}$$

The expression for $\hat{\Gamma}_{(\text{II})}^{(3)}$ agrees with [7] (which is based on the calculations done in [20]) up to a constant factor due to normalization convention, and the expression for $\hat{\Gamma}_{(\text{I})}^{(3)}$ agrees with $\hat{\Gamma}_{(\text{II})}^{(3)}$ when $c_{\mathbf{q},\mathbf{r}} = -1$. In the rigid case, these expressions are again found to agree with [7] up to normalization, though they are not explicitly shown here.

3.4 The Evolution Equation

The evolution equation truncated to leading order is therefore

$$\partial_t A_{\mathbf{k}} = (\sigma_0 + \sigma_2 (k^2 - k_c^2)^2) A_{\mathbf{k}} + \iiint_{(II)} \Gamma_{\mathbf{k}}^{(3)}(\mathbf{p}, \mathbf{q}, \mathbf{r}) A_{\mathbf{p}} A_{\mathbf{q}} A_{\mathbf{r}} d\mathbf{p} d\mathbf{q} d\mathbf{r},$$

where (13)-(14) have been used, the kernel is given in (34), and the integration is done in case (II) of (33). If the deviation from the marginal Rayleigh number scales as $\sigma_0 \sim \epsilon^2$, consistent scalings near marginality are $\partial_t \sim \epsilon^2$, $k^2 - k_c^2 \sim \epsilon$, $A \sim \epsilon$. In the physical space, with additional re-scaling of t and x, we finally have the nonlocal pattern equation

$$\partial_t u = ru - (\Delta + k_0^2)^2 u + \iiint_{(II)} \hat{\Gamma}^{(3)}(\varpi, c_{\mathbf{q},\mathbf{r}}) e^{i(\mathbf{p}+\mathbf{q}+\mathbf{r})\cdot\mathbf{x}} u_{\mathbf{p}} u_{\mathbf{q}} u_{\mathbf{r}} d\mathbf{p} d\mathbf{q} d\mathbf{r}, \qquad (37)$$

where all the coefficients are $O(1)$.

For 2D convection, $\mathbf{p}$, $\mathbf{q}$ and $\mathbf{r}$ are constrained to be collinear, so $\hat{\Gamma}^{(3)}$ reduces to a constant, and (37) reduces to the 1D Swift-Hohenberg equation [23]

$$\partial_t u = ru - (\Delta + k_0^2)^2 u + f_3 u^3, \qquad (38)$$

where f_3 is a constant depending on ϖ. The usual Swift-Hohenberg model for the standard Rayleigh-Bénard convection problem has had a remarkable qualitative success in reproducing the gamut of observed patterns in the Boussinesq context. However, to make quantitative comparison between theory and experiment a nonlocal pattern equations such as the one found here and in earlier discussions (e.g. [19]) may be called for. At any rate, our analysis indicates that the constant part of the kernel $\hat{\Gamma}_{(I)}^{(3)}$ does yield a local cubic term in the evolution equation, but the nonconstant part leads to nonlocal interactions.

4 The Variational Structure and Its Applications

An evolution equation $\partial_t u = M[u]$ is called variational if it can be written

$$\partial_t u = -\delta \mathcal{F}/\delta u,$$

where $\delta \mathcal{F}/\delta u$ is the functional (or Fréchet) derivative. It may then be shown that $d\mathcal{F}/dt \le 0$. If, in addition, $\mathcal{F}[u]$ is bounded from below, it is called a Lyapunov functional and functions u that minimize it are stable. It is known that (38) has a Lyapunov functional (cf. §4.2.1) and so does (37), under suitable restrictions, as we next see.

4.1 Variational Structure of the Nonlocal Pattern Equation

To find the Lyapunov functional for (37), we seek

$$\mathcal{G}[u] = \iiiint_{(II)} \Lambda(\varpi, c_{\mathbf{q},\mathbf{r}}) \delta(\mathbf{p} + \mathbf{q} + \mathbf{r} + \mathbf{s}) u_{\mathbf{p}} u_{\mathbf{q}} u_{\mathbf{r}} u_{\mathbf{s}} d\mathbf{p} d\mathbf{q} d\mathbf{r} d\mathbf{s}$$

such that

$$\frac{\delta \mathcal{G}}{\delta u} = \iiint_{(II)} \hat{\Gamma}^{(3)}(\varpi, c_{\mathbf{q},\mathbf{r}}) e^{i(\mathbf{p}+\mathbf{q}+\mathbf{r})\cdot\mathbf{x}} u_{\mathbf{p}} u_{\mathbf{q}} u_{\mathbf{r}} d\mathbf{p} d\mathbf{q} d\mathbf{r},$$

where out of the three equivalent scenarios

$$\text{(I)}\, \mathbf{s} = -\mathbf{p},\, \mathbf{q} = -\mathbf{r}; \quad \text{(II)}\, \mathbf{s} = -\mathbf{q},\, \mathbf{r} = -\mathbf{p}; \quad \text{(III)}\, \mathbf{s} = -\mathbf{r},\, \mathbf{p} = -\mathbf{q},$$

we assume that the integration for $\mathcal{G}$ is done in case (II).

After some manipulations with functional derivatives and Fourier transforms, we get

$$\frac{\delta \mathcal{G}}{\delta u} = \iiint_{(II)} \frac{1}{\pi^2} \Lambda(\varpi, c_{\mathbf{q},\mathbf{r}}) e^{i(\mathbf{p}+\mathbf{q}+\mathbf{r})\cdot\mathbf{x}} u_{\mathbf{p}} u_{\mathbf{q}} u_{\mathbf{r}} d\mathbf{p} d\mathbf{q} d\mathbf{r},$$

in light of $c_{\mathbf{q},\mathbf{r}} = c_{\mathbf{r},\mathbf{q}} = c_{\mathbf{p},\mathbf{s}} = c_{\mathbf{s},\mathbf{p}}$. Therefore we should pick

$$\Lambda(\varpi, c_{\mathbf{q},\mathbf{r}}) = \pi^2 \hat{\Gamma}^{(3)}(\varpi, c_{\mathbf{q},\mathbf{r}}). \tag{39}$$

The Lyapunov functional for (37) is

$$\mathcal{F}[u] = \int \left(-\frac{1}{2} r u^2 + \frac{1}{2}((\nabla^2 + k_0^2)u)^2 \right) d\mathbf{x} - \mathcal{G}[u]. \tag{40}$$

To show that $\mathcal{F}[u]$ is bounded from below, note that $u_{-\mathbf{k}} = u_{\mathbf{k}}^*$ leads to

$$u_{\mathbf{p}} u_{\mathbf{q}} u_{\mathbf{r}} u_{\mathbf{s}} = |u_{\mathbf{p}}|^2 |u_{\mathbf{q}}|^2 \geq 0.$$

In addition, (35,36,39) imply that (note that $\hat{\Gamma}^{(3)}_{(II)}$ is always non-positive)

$$-\Lambda(\varpi, c_{\mathbf{q},\mathbf{r}}) \geq \pi^2 \frac{\varpi}{4(1+\varpi)} \equiv \pi^2 M > 0.$$

Therefore, we can establish the estimate (now the integration is done over all three cases)

$$-\mathcal{G}[u] \geq \frac{\pi^2 M}{3} \iiiint \delta(\mathbf{p}+\mathbf{q}+\mathbf{r}+\mathbf{s}) u_{\mathbf{p}} u_{\mathbf{q}} u_{\mathbf{r}} u_{\mathbf{s}} d\mathbf{p} d\mathbf{q} d\mathbf{r} d\mathbf{s} = \frac{M}{12} \int u^4 d\mathbf{x},$$

where the identity $u_{\mathbf{s}} = \frac{1}{(2\pi)^2} \int u e^{-i\mathbf{s}\cdot\mathbf{x}} d\mathbf{x}$ is used. It then follows from (40) that

$$\mathcal{F}[u] \geq \int \left(-\frac{1}{2} r u^2 + \frac{1}{2}((\nabla^2 + k_0^2)u)^2 + \frac{M}{12} u^4 \right) d\mathbf{x} \equiv \tilde{\mathcal{F}}[u],$$

where $\tilde{\mathcal{F}}[u]$ is nothing but the Lyapunov functional for (38) with $f_3 = -M/3$. It is known (cf. [11] §7.3) that $\tilde{\mathcal{F}}[u]$ is bounded from below for $f_3 < 0$, so our claim is proved.

We expect the nonlocal pattern equation (37) to accurately capture the physics, but PDE models like (38) enjoy much greater popularity because of their mathematical simplicity. Hence in the following, we derive a few lesser known properties of steady states in dissipative PDE with Lyapunov functionals, and provide a few examples. In terms of notation, repeated Latin indices are summed over, but Greek indices are not.

In general, consider any system in d spatial dimensions with a Lyapunov functional

$$\mathcal{F}[u] = \int \mathcal{L}(u, \partial_i u, \Delta u) d\mathbf{x} \equiv \int \mathcal{L}(q, \mathbf{p}_i, r) d\mathbf{x}, \quad \mathbf{x} \in \mathbb{R}^d.$$

We will focus on $u(\mathbf{x})$ that locally minimizes $\mathcal{F}[u]$, although the equalities that appear below also apply to other stationary points of $\mathcal{F}[u]$ (i.e. saddles and maxima).

4.2 Generalized Virial Theorem

We generalize upon [9] §4 to derive an analog of virial theorem. If we introduce a parameter λ and define $\mathcal{F}(\lambda) \equiv \mathcal{F}[u(\mathbf{x} + \lambda\mathbf{y}(\mathbf{x}))]$, then stationarity and minimality require

$$\mathcal{F}'(\lambda = 0) = 0, \tag{41}$$

$$\mathcal{F}''(\lambda = 0) \geq 0. \tag{42}$$

Consider a linear function $\mathbf{y}(\mathbf{x})$, for which the Jacobian matrix $\mathbf{J}$ (defined by $\mathbf{J}_{ij} \equiv \partial\mathbf{y}_j/\partial\mathbf{x}_i$) is a constant matrix independent of $\mathbf{x}$. For any λ, we can transform the coordinate by $\mathbf{x} + \lambda\mathbf{y}(\mathbf{x}) \to \mathbf{x}$ to obtain the exact expression

$$\mathcal{F}(\lambda) = \int \frac{\mathcal{L}(u, \partial_i u + \lambda\mathbf{J}_{ij}\partial_j u, \Delta u + \lambda(\mathbf{J}_{jk} + \mathbf{J}_{kj})\partial_{jk}u + \lambda^2\mathbf{J}_{ij}\mathbf{J}_{ik}\partial_{jk}u)}{\det(\mathbf{I} + \lambda\mathbf{J})}d\mathbf{x}, \tag{43}$$

where $\mathbf{I}$ is the identity matrix. Here the integration domain is left unspecified, but certain conditions near the boundary must be satisfied. As a simple example from calculus, for an arbitrary function $\varphi(x)$

$$\int_0^L \varphi(\lambda x)d(\lambda x) = \int_0^{L/\lambda} \varphi(x)dx \neq \int_0^L \varphi(x)dx$$

unless $\varphi(x) \to 0$ at $x \to L$. Therefore, we may either take a finite domain and require $\mathcal{L} = 0$ near the boundary, or take the domain to be $\mathbb{R}^d$ and require $\mathcal{L} \in L^1(\mathbb{R}^d)$. In other words, what follows should be applied to steady localized states with bounded total free energy.

We see that in (43), λ and $\mathbf{J}$ always appear as the combination $\lambda\mathbf{J}$, so $\mathcal{F}^{(n)}(\lambda = 0)$ must be n-linear in $\mathbf{J}$. For $|\lambda| \ll 1$, the denominator can be expanded as

$$\det(\mathbf{I} + \lambda\mathbf{J}) = \exp(\text{tr}(\log(\mathbf{I} + \lambda\mathbf{J}))) = \sum_{k=0}^{\infty} \frac{1}{k!}\left(-\sum_{j=1}^{\infty}\frac{(-\lambda)^j}{j}\text{tr}(\mathbf{J}^j)\right)^k,$$

from which follows the useful expression

$$\frac{1}{\det(\mathbf{I} + \lambda\mathbf{J})} = 1 - \lambda\text{tr}\mathbf{J} + \frac{\lambda^2}{2}(\text{tr}^2\mathbf{J} + \text{tr}\mathbf{J}^2) + O(\lambda^3).$$

Since $\mathcal{F}'(\lambda = 0)$ is linear in $\mathbf{J}$, we only need to impose (41) on the following two classes of transformations. The first is the class of scaling transforms $\mathbf{J}_{ij} = \delta_{i\mu}\delta_{j\mu}$, which leads to

$$\int \left(\mathcal{L}_{\mathbf{p}_\mu}\partial_\mu u + 2\mathcal{L}_r\partial_{\mu\mu}u - \mathcal{L}\right)d\mathbf{x} = 0, \tag{44}$$

Summation over μ yields the "global" virial theorem

$$\int \left(\mathcal{L}_{\mathbf{p}} \cdot \mathbf{p} + 2\mathcal{L}_r r - d\mathcal{L}\right)d\mathbf{x} = 0,$$

or equivalently (in fact, more generally)

$$\sum_i (i - d)\int \mathcal{L}_i d\mathbf{x} = 0, \tag{45}$$

where $\mathcal{L}_i$ is the term in $\mathcal{L}$ with i spatial derivatives in total. The second is the class of shear transforms $\mathbf{J}_{ij} = \delta_{i\mu}\delta_{j\nu}$ ($\mu \neq \nu$), which leads to

$$\int \left(\mathcal{L}_{\mathbf{p}_\mu}\partial_\nu u + 2\mathcal{L}_r\partial_{\mu\nu}u\right)d\mathbf{x} = 0, \tag{46}$$

We may summarize (44) and (46) as an orthogonality condition (μ and ν are arbitrary)

$$\boxed{\int(\mathcal{L}_{\mathbf{p}_\mu} + 2\mathcal{L}_r\partial_\mu)\partial_\nu u\,d\mathbf{x} = \delta_{\mu\nu}\int\mathcal{L}d\mathbf{x}.} \tag{47}$$

Since $\mathcal{F}''(\lambda = 0)$ is a quadratic form in the matrix elements $\mathbf{J}_{ij}$, (42) is equivalent to the requirement that the $d^2 \times d^2$ matrix

$$\mathbf{H}_{\kappa\lambda\mu\nu} = \int(\mathcal{L}\left(\delta_{\kappa\lambda}\delta_{\mu\nu} + \delta_{\kappa\nu}\delta_{\lambda\mu}\right) + 2\mathcal{L}_r(\delta_{\kappa\mu}\partial_{\lambda\nu}u - 2\delta_{\kappa\lambda}\partial_{\mu\nu}u) - 2\mathcal{L}_{\mathbf{p}_\mu}\delta_{\kappa\lambda}\partial_\nu u$$
$$+4\mathcal{L}_{rr}\partial_{\kappa\lambda}u\partial_{\mu\nu}u + 4\mathcal{L}_{r\mathbf{p}_\mu}\partial_\nu u\partial_{\kappa\lambda}u + \mathcal{L}_{\mathbf{p}_\mu\mathbf{p}_\kappa}\partial_\nu u\partial_\lambda u)d\mathbf{x},$$

defined such that $\mathcal{F}''(\lambda = 0) = \mathbf{J}_{kl}\mathbf{H}_{klmn}\mathbf{J}_{mn}$, is nonnegative definite. However, we cannot see any immediate application of this result, except in the special case $\mathbf{J}_{ij} = \delta_{ij}$. Then

$$\mathcal{F}''(\lambda = 0) = \int \left(d(d+1)\mathcal{L} + 2(1-2d)\mathcal{L}_r r - 2d\mathcal{L}_{\mathbf{p}}\cdot\mathbf{p} + 4\mathcal{L}_{rr}r^2 + 4\mathcal{L}_{r\mathbf{p}}\cdot\mathbf{p}r + \mathcal{L}_{\mathbf{p}_i\mathbf{p}_j}\mathbf{p}_i\mathbf{p}_j\right)d\mathbf{x} \geq 0,$$

or equivalently (in fact, more generally)

$$\mathcal{F}''(\lambda = 0) = \sum_i (i-d)(i-d-1)\int\mathcal{L}_i d\mathbf{x} \geq 0. \tag{48}$$

4.2.1 Applications

Let us introduce the shorthand $I_i \equiv \int\mathcal{L}_i d\mathbf{x}$. Sometimes, (45) and (48) together with the positivity (or negativity) of I_i can be restated as a linear programming problem. The nonexistence of solutions for I_i then implies the nonexistence of stable localized states.

To take an example, the generalized Swift-Hohenberg equation

$$\frac{\partial u}{\partial t} = ru - (\nabla^2 + k_0^2)^2 u + f(u), \tag{49}$$

where the nonlinear function f may be either quadratic-cubic or cubic-quintic in u, has a Lyapunov functional with free energy density

$$\mathcal{L}^{SH} = -\frac{1}{2}ru^2 + \frac{1}{2}((\nabla^2 + k_0^2)u)^2 - F(u), \quad F' = f.$$

For another example, the steady state Proctor equation [18]

$$0 = \mu^2\nabla^2 u + \nabla^4 u - \nabla\cdot(|\nabla u|^2\nabla u) + \beta u, \quad \beta > 0 \tag{50}$$

has a Lyapunov functional with free energy density

$$\mathcal{L}^P = \frac{1}{4}|\nabla u|^4 + \frac{1}{2}|\nabla^2 u|^2 - \frac{\mu^2}{2}|\nabla u|^2 + \frac{\beta}{2}u^2.$$
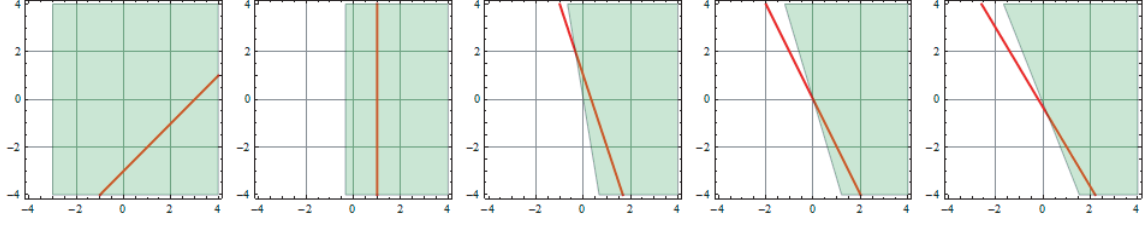
Figure 3: The R_0(horizontal)-R_2(vertical) plane. (45)/(48) defines the solid line/shaded region. Their intersection forms the segment of possible stable localized states. From left to right, d varies from 1 to 5, whereas $d \geq 6$ is qualitatively the same as $d = 5$.

The free energies for both (49) and (50) consist of I_0, I_2 and $I_4 > 0$. Hence we may introduce $R_i = I_i/I_4$ ($i = 0, 2$), and rewrite (45) and (48) as

$$(4-d) + (2-d)R_2 + (-d)R_0 = 0, \quad (4-d)(3-d) + (2-d)(1-d)R_2 + (-d)(-1-d)R_0 \geq 0.$$

The segment that they define on the R_0-R_2 plane depends on d (Fig. 3). In addition

$$I_2^{SH} = k_0^2 \int \left(u\nabla^2 u\right) d\mathbf{x} = -k_0^2 \int |\nabla u|^2 d\mathbf{x} < 0, \quad I_2^P = -\frac{\mu^2}{2} \int |\nabla u|^2 d\mathbf{x} < 0.$$

As for I_0, we have

$$I_0^{SH} \geq C \int u^2 d\mathbf{x}, \quad I_0^P = \frac{\beta}{2} \int u^2 d\mathbf{x} > 0,$$

where $C > 0$ for some choices of parameters. These inequalities imply that both (49) and (50) can possibly have stable localized solutions for any d. One can make a better estimate for R_0 from the Cauchy-Schwarz inequality

$$\left| \int \left(u\nabla^2 u\right) d\mathbf{x} \right| \leq \left(\int u^2 d\mathbf{x} \right)^{1/2} \left(\int |\nabla^2 u|^2 d\mathbf{x} \right)^{1/2}.$$

This further shortens the segment on the R_0-R_2 plane, but does not change the conclusion.

It is necessary that the PDE takes the precise form $u_t = -\delta \mathcal{F}/\delta u$. As an example to the contrary, the Cahn-Hilliard equation [3]

$$\partial_t u = \Delta(u^3 - u - \gamma \Delta u), \quad \gamma > 0 \tag{51}$$

has a Lyapunov functional with free energy density

$$\mathcal{L}^{CH} = \frac{1}{4}(u^2 - 1)^2 + \frac{\gamma}{2}|\nabla u|^2,$$

such that $u_t = \Delta(\delta \mathcal{F}/\delta u)$ where $\mathcal{F} = \int \mathcal{L}^{CH} d\mathbf{x}$. Stable localized solutions to (51) must satisfy $\delta \mathcal{F}/\delta u = 0$, but are not necessarily local minima of $\mathcal{F}[u]$. For example, a spherical *bubble* of $u = -1$ with any finite radius, embedded in a $u = 1$ background, is stable. We could decrease $\mathcal{F}$ by shrinking the bubble radially, but this is forbidden since it violates

$$\frac{d}{dt} \int u d\mathbf{x} = 0,$$

a conservation law that follows from (51) rewritten as

$$\partial_t u = \nabla \cdot \mathbf{j} \quad \text{with} \quad \mathbf{j} = \nabla(u^3 - u - \gamma \Delta u).$$

We refer the reader to [8] for such reasoning applied to nonlinear wave equations.

4.3 Least Action Principle

Consider a finite spatial domain $\mathcal{D}$. The change in free energy under perturbation δu is

$$\delta \mathcal{F} = \mathcal{F}[u + \delta u] - \mathcal{F}[u] = \int_{\partial \mathcal{D}} (\mathcal{L}_r \nabla \delta u + \delta u (\mathcal{L}_\mathbf{p} - \nabla \mathcal{L}_r)) \cdot \hat{n} dA - \int_{\mathcal{D}} H \delta u d\mathbf{x}, \qquad (52)$$

where $H = -\mathcal{L}_q + \partial_i \mathcal{L}_{\mathbf{p}_i} - \Delta \mathcal{L}_r$, $\partial \mathcal{D}$ is the boundary of $\mathcal{D}$, $\hat{n}$ is the unit outward normal to $\partial \mathcal{D}$ and dA is the surface element on $\partial \mathcal{D}$. If (52) is to vanish for arbitrary δu, $H = 0$ must be satisfied on $\mathcal{D}$, and in addition the following boundary conditions must be fulfilled

$$\boxed{\mathcal{L}_r = 0, \quad (\mathcal{L}_\mathbf{p} - \nabla \mathcal{L}_r) \cdot \hat{n} = 0 \quad \text{on} \quad \partial \mathcal{D}.}$$

4.3.1 Applications

For the Swift-Hohenberg equation, the boundary conditions are (here $\mathcal{L}_r = (\nabla^2 + k_0^2)u$)

$$\mathcal{L}_r = 0, \quad \nabla \mathcal{L}_r \cdot \hat{n} = 0 \quad \text{on} \quad \partial \mathcal{D}.$$

These conditions require that at the boundary, both u and $\nabla u \cdot \hat{n}$ must have planform wavelengths k_0. However, if the convection rolls merge perpendicularly with the boundary, then $\nabla u \cdot \hat{n} = 0$ and only the constraint on u remains. This is a plausible reason why such behavior is most often observed in convection experiments near the onset of instability.

For a more quantitative approach to the roll merging problem, we refer the reader to [26].

4.4 A Conservation Law

According to [14], for any $\mathcal{L}$ not explicitly dependent on $\mathbf{x}$, we have the conservation law

$$\partial_{x_1} \mathcal{L} - \nabla \cdot (u_{x_1} \mathcal{L}_\mathbf{p} + \mathcal{L}_r \nabla u_{x_1} - u_{x_1} \nabla \mathcal{L}_r) = 0 \quad \text{for all} \quad \mathbf{x} \in \mathbb{R}^d, \qquad (53)$$

where ∂_{x_1} can be replaced by any other directional derivative. To interpret (53) physically, we make a perturbation δu proportional to u_{x_1}. In view of (52), the second term of (53) is the local contribution to the bilinear concomitant, or equivalently the free energy flux. On the other hand, the perturbation essentially translates u in the $-x_1$ direction, so the free energy flux can also be expressed as the first term of (53). Thus, (53) is a consequence of the special choice of perturbation by a translational mode.

4.4.1 Applications

For $d = 2$ in the Swift-Hohenberg equation, (53) is directly responsible for selecting the wavelength of hexagonal pattern that connects through a front to the trivial state [14]. For the PDE studied in [9], however, (53) simply reduces to the original PDE.

5 Normal Forms of Pattern Equations

In bifurcation theory for ODE, (24) and (25) in §3.2 represent two steps of reduction [22]. In the first step (center manifold reduction), the power series corresponding to (25) is uniquely determined but in terms of the *original* center manifold coordinate (denoted by $\boldsymbol{\alpha}$). This results in an evolution equation for $\boldsymbol{\alpha}$

$$\frac{d\boldsymbol{\alpha}}{dt} = \mathbb{M}\boldsymbol{\alpha} + \boldsymbol{\Gamma}(\boldsymbol{\alpha}), \tag{54}$$

where $\boldsymbol{\Gamma}(\boldsymbol{\alpha})$ is purely nonlinear in $\boldsymbol{\alpha}$. The matrix $\mathbb{M}$ depends only on the control parameters, with its eigenvalues having real parts all equal to 0 at criticality. In the second step (normal form theory), we choose a near-identity coordinate change corresponding to (24)

$$\boldsymbol{\alpha} = \mathbf{A} + \boldsymbol{\Psi}(\mathbf{A}),$$

where $\mathbf{A}$ is the *new* center manifold coordinate, and $\boldsymbol{\Psi}(\mathbf{A})$ is purely nonlinear in $\mathbf{A}$. The purpose is to simplify the nonlinear term $\boldsymbol{\Gamma}(\boldsymbol{\alpha})$ in (54) as much as possible. In the end we obtain an evolution equation for $\mathbf{A}$

$$\frac{d\mathbf{A}}{dt} = \mathbb{M}\mathbf{A} + \mathbf{g}(\mathbf{A}), \tag{55}$$

where $\mathbf{g}(\mathbf{A})$ represents the simplified nonlinear terms. It can be shown that (55), the (not necessarily unique) normal form, depends only on $\mathbb{M}$ (cf. [6]), and is therefore universal for all bifurcations with the same linear part.

In §3.2, the PDE model actually undergoes a pitchfork bifurcation at finite wavenumber. It is known that normal form theory cannot simplify the nonlinear terms for steady state bifurcations, which is why we can identify the new center manifold coordinate F with the original coordinate f. In this section, however, we derive the normal form of pattern equation for Hopf bifurcation, the simplest situation where normal form theory is necessary.

5.1 Hopf Bifurcation

Consider a physical system with an active control parameter λ, like the Rayleigh-Bénard convection, but whose critical modes are a pair of complex conjugate normal modes $(\phi_\mathbf{k}, \phi_\mathbf{k}^*)$ with growth rates $(\mu_\mathbf{k} + i\omega_\mathbf{k}, \mu_\mathbf{k} - i\omega_\mathbf{k})$, where $\mathbf{k}$ is the horizontal wave vector. This pair of critical modes loses stability, that is, $\mu_\mathbf{k}$ crosses through 0, at a critical wavenumber $|\mathbf{k}| = k_c$ as λ crosses through a critical value λ_c. We assume that all the other normal modes remain linearly stable when λ is near λ_c.

We expect that the dynamics is captured by the amplitudes of the pair of critical modes $(\phi_\mathbf{k}, \phi_\mathbf{k}^*)$, which are denoted by $(\alpha_\mathbf{k}, \alpha_\mathbf{k}^*)$. Hence we may utilize the Bogoliubov method to derive the following amplitude equation for λ near λ_c and $|\mathbf{k}|$ near k_c

$$\partial_t \alpha_\mathbf{k} = (\mu_\mathbf{k} + i\omega_\mathbf{k})\alpha_\mathbf{k} + \Gamma_\mathbf{k}[\alpha_\mathbf{p}, \alpha_\mathbf{q}^*], \tag{56}$$

where $\Gamma_\mathbf{k}$ is a purely nonlinear functional power series of $\alpha_\mathbf{p}$ and $\alpha_\mathbf{q}^*$, which possibly contains nonlocal interactions. The amplitude $\alpha_\mathbf{k}^*$ satisfies the complex conjugate of (56). In normal form theory, we try to simplify (56) by the near-identity coordinate change

$$\alpha_\mathbf{k} = A_\mathbf{k} + \Psi_\mathbf{k}[A_\mathbf{p}, A_\mathbf{q}^*],$$

so that $A_{\mathbf{k}}$ satisfies

$$\partial_t A_{\mathbf{k}} = (\mu_{\mathbf{k}} + i\omega_{\mathbf{k}})A_{\mathbf{k}} + g_{\mathbf{k}}[A_{\mathbf{p}}, A_{\mathbf{q}}^*].$$

The equation for $\Psi_{\mathbf{k}}$ is found by substitution into (56) to be

$$\mathcal{L}_{\mathbf{k}}\Psi_{\mathbf{k}} = T_{\mathbf{k}} - g_{\mathbf{k}} \tag{57}$$

where the linear operator is

$$\mathcal{L}_{\mathbf{k}}\Psi_{\mathbf{k}} = \int \frac{\delta\Psi_{\mathbf{k}}}{\delta A_{\mathbf{p}}}(\mu_{\mathbf{p}} + i\omega_{\mathbf{p}})A_{\mathbf{p}}d\mathbf{p} + \int \frac{\delta\Psi_{\mathbf{k}}}{\delta A_{\mathbf{q}}^*}(\mu_{\mathbf{q}} - i\omega_{\mathbf{q}})A_{\mathbf{q}}^*d\mathbf{q} - (\mu_{\mathbf{k}} + i\omega_{\mathbf{k}})\Psi_{\mathbf{k}}$$

and the nonlinear term has been abbreviated by

$$T_{\mathbf{k}} = \Gamma_{\mathbf{k}}[A_{\mathbf{p}} + \Psi_{\mathbf{p}}, A_{\mathbf{q}}^* + \Psi_{\mathbf{q}}^*] - \int \frac{\delta\Psi_{\mathbf{k}}}{\delta A_{\mathbf{p}}}g_{\mathbf{p}}d\mathbf{p} - \int \frac{\delta\Psi_{\mathbf{k}}}{\delta A_{\mathbf{q}}^*}g_{\mathbf{q}}^*d\mathbf{q}. \tag{58}$$

The functional power series above are formed by monomials conveniently denoted as

$$\begin{aligned}
|DK\rangle_{\mathcal{Q}} &= \left(\prod_{i=1}^{D-K}\int d\mathbf{p}_i\right)\left(\prod_{j=1}^{K}\int d\mathbf{q}_j\right)\mathcal{Q}_{DK}(\mathbf{p}_1, \cdots, \mathbf{p}_{D-K}, \mathbf{q}_1, \cdots, \mathbf{q}_K) \\
&\times \; \delta\left(\sum_{i=1}^{D-K}\mathbf{p}_i + \sum_{j=1}^{K}\mathbf{q}_j - \mathbf{k}\right)\prod_{i=1}^{D-K}A_{\mathbf{p}_i}\prod_{j=1}^{K}A_{\mathbf{q}_j}^*,
\end{aligned} \tag{59}$$

where $\mathcal{Q} = \Psi$, g or T. When the kernel $\mathcal{Q}_{DK}$ is constant (denoted by $\bar{\mathcal{Q}}_{DK}$), the monomial $|DK\rangle_{\mathcal{Q}}$ reduces to the local expression $\bar{\mathcal{Q}}_{DK}(A^{D-K}(A^*)^K)_{\mathbf{k}}$. It may seem that in (59) we need to deal with two fields $A_{\mathbf{k}}$ and $A_{\mathbf{k}}^*$, but the relation $A_{\mathbf{k}}^* = A_{-\mathbf{k}}$ suggests that A^* can be transformed to A by reversal of wave vector. Therefore, we may choose to represent $|DK\rangle_{\mathcal{Q}}$ by a diagram with $D - K$ lines with right arrows and K lines with left arrows, both connected to a vertex labelled $\mathcal{Q}$. We can use these two notations interchangeably, e.g.

$$|31\rangle_{\Gamma} \quad \Leftrightarrow \quad \text{⬤⬤⬤}\!\!\!\!\!\!\!\!\!\!\Rightarrow\!\!\!\Gamma \quad .$$

Regardless of the kernel $\mathcal{Q}_{DK}$, any monomial is an eigenvector of $\mathcal{L}_{\mathbf{k}}$

$$\mathcal{L}_{\mathbf{k}}|DK\rangle_{\mathcal{Q}} = \Lambda_{DK}|DK\rangle_{\mathcal{Q}}$$

if we take $A_{\mathbf{k}}$ to have infinitesimal support around $|\mathbf{k}| = k_c$. The eigenvalue is

$$\Lambda_{DK} = i\omega_{k_c}(D - 2K - 1) + \mu_{k_c}(D - 1). \tag{60}$$

Then (57) becomes

$$\Lambda_{DK}|DK\rangle_{\Psi} = |DK\rangle_T - |DK\rangle_g \tag{61}$$

for $D \geq 2$. From (58) we know $|2K\rangle_T$, so we can solve (61) when $D = 2$, once we choose $|2K\rangle_g$. Thereafter, at each new D, $|DK\rangle_T$ is known if we solve sequentially.

As long as $\Lambda_{DK} \neq 0$, we can always choose $g_{DK} = 0$. However, (60) suggests that when $\mu_{k_c} = 0$ (i.e. $\lambda = \lambda_c$), Λ_{DK} vanishes when $K = (D-1)/2$, or equivalently $\Lambda_{2L+1,L} = 0$ for

$L = 1, 2, \cdots$. To avoid the small denominator $\Lambda_{2L+1,L}$ near λ_c, we require that $g_{2L+1,L} = T_{2L+1,L}$. All the other g_{DK} may be set equal to 0. Therefore the normal form is

$$\partial_t A_\mathbf{k} = (\mu_\mathbf{k} + i\omega_\mathbf{k})A_\mathbf{k} + |31\rangle_T + |52\rangle_T + \cdots . \tag{62}$$

The diagrammatic notation is not needed to get (62), but it can be useful for calculating the normal form "coefficients" T_{31}, T_{52}, etc. As an example, to expand the convolution $\int(\delta\Psi_\mathbf{k}/\delta A_\mathbf{p})g_\mathbf{p}d\mathbf{p}$ in (58), we first cross out any of the $D - K$ instances of A that occur in $|DK\rangle_\Psi$, which results in $D - K$ diagrams with an empty slot each. Then we fill each slot with the functional power series $g_\mathbf{p}$, and sum up these $D - K$ diagrams in the end.

Overall, the above normal form theory for Hopf bifurcation in nonlocal pattern equation parallels the ODE case (cf. [22] §4). We will not study the properties of (62), but mention that when T_{31} is constant and $k_c = 0$, (62) truncated to third order is the complex Ginzburg-Landau equation (CGLE), whose solutions have been extensively documented [1]. The CGLE, or more generally (62), is invariant under the phase-shift $A \to Ae^{i\phi}$ where ϕ is a constant. Interestingly, in terms of diagrams, we may assign A (A^*) spin $1/2$ $(-1/2)$, and state this invariance as the conservation of total spin among all diagrams.

6 Conclusion

In this report, we derived a nonlocal pattern equation for Rayleigh-Bénard convection with fixed temperature boundaries, found a Lyapunov functional for this equation, and then formulated a few properties of steady state solutions of variational PDE. The diagrammatic technique proved instrumental in the derivation of convective pattern equations.

There exist unresolved issues and open questions. First, for Rayleigh-Bénard convection, it remains to find a suitable way of removing the singularities that come from resonances among fast and slow modes (cf. §3.2). Second, we need to interpret the generalized virial theorem physically, and work out more applications. It is also interesting to study how these properties of variational PDE generalize to nonlocal pattern equations. Finally, we plan to extend [22] §5 on multiple instabilities to nonlocal pattern equation. However, for higher codimension bifurcations, even if center manifold reduction works as before, it is not clear how normal form theory can be formulated. In this case, the linear term does not uniquely determine the nonlinear terms that cannot be discarded in the normal form.

Acknowledgement

References

[1] **The world of the complex Ginzburg-Landau equation**, ARANSON, I. S. AND KRAMER, L. 2002, *Rev. Mod. Phys.*, **Vol. 74 No. 1**, 99-143.

[2] **Energy transfer between external and internal gravity waves**, BALL, F. K. 1964, *J. Fluid Mech.*, **19**, 465-478.

[3] **Free energy of a nonuniform system. I. Interfacial free energy**, CAHN, J. W. AND HILLIARD, J. E. 1958, *J. Chem. Phys.*, **28**, 258-267.

[4] **Hydrodynamic and hydromagnetic stability**, CHANDRASEKHAR, S. 1961, *Oxford: Clarendon Press.*

[5] **Evolution equations for extended systems**, COULLET, P. H. AND SPIEGEL, E. A. 1987, in *Energy stability and convection*, Pitman Research Notes 168, edited by G. P. Galdi and B. Straughan (Wiley, New York).

[6] **Introduction to bifurcation theory**, CRAWFORD, J. D. 1991, *Rev. Mod. Phys.*, **Vol. 63 No. 4**, 991-1037.

[7] **Derivation of the amplitude equation at the Rayleigh-Bénard instability**, CROSS, M. C. 1980, *Phys. Fluids*, **23**(9), 1727-1731.

[8] **Comments on nonlinear wave equations as models for elementary particles**, DERRICK, G. H. 1964, *J. Math. Phys.*, **Vol. 5 No. 9**, 1252-1254.

[9] **Complexity from thermal instability**, ELPHICK, C., REGEV, O. AND SPIEGEL, E. A. 1991, *Mon. Not. R. Astr. Soc.*, **250**, 617-628.

[10] **Wave propagation in random media**, FRISCH, U. 1968, in *Probabilistic methods in applied mathematics*, edited by A. T. Bharucha-Reid (Academic, New York).

[11] **Pattern Formation**, HOYLE, R. 2006, *Cambridge University Press.*

[12] **Classical Dynamics: A Contemporary Approach**, JOSE, J. V. AND SALETAN, E. J. 1998, *Cambridge University Press.*

[13] **Fluid Mechanics**, KUNDU, P. K. AND COHEN, I. M. 2007, *Academic Press.*

[14] **Localized hexagon patterns of the planar Swift-Hohenberg equation**, LLOYD, D. J. B., SANDSTEDE, B., AVITABILE, D. AND CHAMPNEYS, A. R. 2008, *SIAM J. Appl. Dyn. Syst.*, **Vol. 7 No. 3**, 1049-1100.

[15] **A Guide to Feynman Diagrams in the Many-Body Problem**, MATTUCK, R. D. 1992, *Dover Publications.*

[16] **An Introduction to Quantum Field Theory**, PESKIN, M. E. AND SCHROEDER, D. V. 1995, *Westview Press.*

[17] **Inertial effects in long-scale thermal convection**, Pismen, L. M. 1986, *Phys. Lett. A*, **Vol. 116 No. 5**, 241-244.

[18] **Planform selection by finite-amplitude thermal convection between poorly conducting slabs**, Proctor, M. R. E. 1981, *J. Fluid Mech.*, **113**, 469-485.

[19] **The Swift-Hohenberg equation requires nonlocal modifications to model spatial pattern evolution of physical problems**, Roberts, A. J. 1994, *Preprint*, arXiv:patt-sol/9412002.

[20] **On the stability of steady finite amplitude convection**, Schlüter, A., Lortz, D. and Busse, F. 1965, *J. Fluid Mech.*, **Vol. 23 Part 1**, 129-144.

[21] **Pattern selection in Rayleigh-Bénard convection near threshold**, Siggia, E. D. and Zippelius, A. 1981, *Phys. Rev. Lett.*, **Vol. 47 No. 12**, 835-838.

[22] **Cosmic arrhythmias**, Spiegel, E. A. 1985, in *Chaos in astrophysics; Proceedings of the Advanced Research Workshop*, Dordrecht, D. Reidel Publishing Co., 91-135.

[23] **Hydrodynamic fluctuations at the convective instability**, Swift, J. and Hohenberg, P. C. 1977, *Phys. Rev. A*, **Vol. 15 No. 1**, 319-328.

[24] **Instability in extended systems**, Tao, L. and Spiegel, E. A. 1993, in *Proceedings of the Summer Study Program in G.F.D.*, Woods Hole Oceanographic Institution, pp. 177-184.

[25] **Formulation of the theory of turbulence in an incompressible fluid**, Wyld, H. W. 1961, *Annals of Physics*, **14**, 143-165.

[26] **Optimal merging of rolls near a plane boundary**, Zaleski, S., Pomeau, Y. and Pumir, A. 1984, *Phys. Rev. A*, **Vol. 29 No. 1**, 366-370.

[27] **Electrons and Phonons**, Ziman, J. M. 1960, *Oxford.*